Muon multiplicities measured using an underground cosmic-ray array

2016 J. Phys.: Conf. Ser. 718 052021

(http://iopscience.iop.org/1742-6596/718/5/052021)

XIV International Conference on Topics in Astroparticle and Underground Physics (TAUP 2015) IOP Publishing
Journal of Physics: Conference Series **718** (2016) 052021 doi:10.1088/1742-6596/718/5/052021

Muon multiplicities measured using an underground cosmic-ray array

P Kuusiniemi[1], T Enqvist[1], L Bezrukov[2], H Fynbo[3], L Inzhechik[4], J Joutsenvaara[1], K Loo[5], B Lubsandorzhiev[2], V Petkov[2], M Slupecki[5], W H Trzaska[5] and A Virkajärvi[1]

[1] Oulu Southern Institute and Department of Physics, University of Oulu, Finland
[2] Institute of Nuclear Research, Russian Academy of Sciences, Moscow, Russia
[3] Department of Physics and Astronomy, Aarhus University, Denmark
[4] Moscow Institute of Physics and Technology, Moscow, Russia
[5] Department of Physics, University of Jyväskylä, Finland

E-mail: pasi.kuusiniemi@oulu.fi

Abstract.
EMMA (Experiment with Multi-Muon Array) is an underground detector array designed for cosmic-ray composition studies around the knee energy (or $\sim 1 - 10$ PeV). It operates at the shallow depth in the Pyhäsalmi mine, Finland. The array consists of eleven independent detector stations ~ 15 m^2 each. Currently seven stations are connected to the DAQ and the rest will be connected within the next few months. EMMA will determine the multiplicity, the lateral density distribution and the arrival direction of high-energy muons event by event. The preliminary estimates concerning its performance together with an example of measured muon multiplicities are presented.

1. Introduction

The most comprehensive investigations of cosmic-ray (CR) composition at the knee region were obtained from the on-ground experiment KASCADE-Grande in Karlsruhe, Germany (see [1] and references therein). As the analysis and conclusions of such experiments depend heavily on models and simulations, it is necessary to confirm the KASCADE-Grande results by using a different approach. For example, underground experiments employ only high-energy muons and reject the dominant electromagnetic component of the extensive CR showers. As the high-energy muons originate from the early phases of the showers, they carry the most vital information about the energy and mass of the primary CR particle. There have been several underground experiments placed deep underground in the past (see, for example, [2, 3, 4, 5, 6]) to study the cosmic-ray composition at the knee region but the outcome of these experiments is inconclusive or needs to be verified.

In order to investigate the problem further we performed CORSIKA simulations [7] which reveal that in showers with muon energy in excess of 50 GeV the muon lateral density distribution is sensitive to the energy and mass of the primary cosmic-ray particle. The primary energy is proportional to the muon density at the shower core, and is somewhat independent on mass, and the gradients of proton- and iron-initiated showers are rather well separated.

This is illustrated in Fig. 1 where the average muon density distributions of 1, 3 and 10 PeV proton- and iron-initiated air showers are shown. Furthermore, a shallow depth is sufficient to filter out all particles but muons while provides better statistics (i.e. more muons) in the tails. In general, for a given primary energy there are more muons produced in iron-induced showers than those of proton. By increasing the overburden the separation between these two groups of events is more pronounced as the low-energy muons in the tail section are removed. The optimum separation depth depends on the primary energy (of the CR). For CR energies from the knee region the muon cutoff energy should be around 50 GeV. Fig. 1 shows the simulated muon densities calculated for the 50 GeV cutoff. The two clear features are visible in the plot: the muon density at the core is a good indication of the primary energy and the slope of the density distribution contains the information on the mass of the primary particle as it is steeper for proton than for iron. These effects do not have a strong model dependence as both QGSJET and EPOS yield virtually the same results. Therefore it seems reasonable to assume that the muon density at the shower core and the muon density gradient in the tails can be used to estimate the energy and mass of primary cosmic rays, respectively.

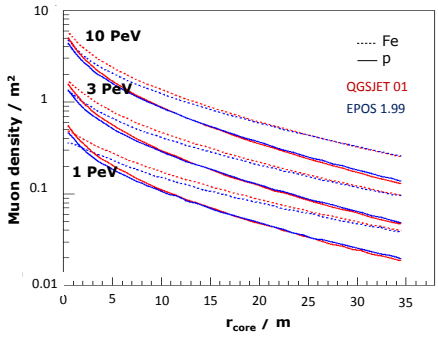

Figure 1. Simulated lateral muon density distributions of high-energy muons ($E_\mu > 50$ GeV) of proton and iron-initiated air showers at 1, 3 and 10 PeV energies using CORSIKA+QGSJET 01 and CORSIKA+EPOS 1.99 indicated by red and blue lines, respectively. The figure is adopted from [8].

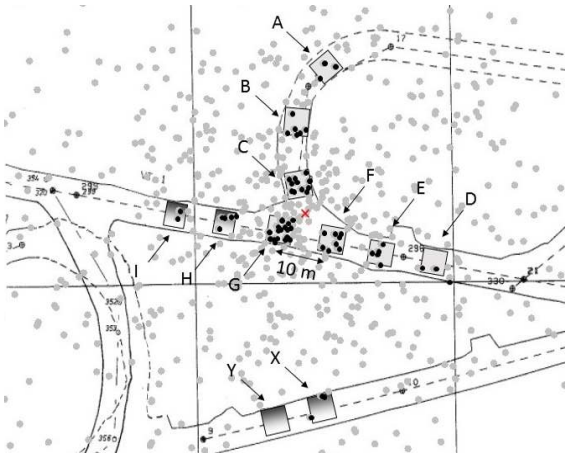

Figure 2. Schematic layout of EMMA at 75 metres below ground ($E_\mu > 50$ GeV) detecting a simulated (CORSIKA+QGSJET 02) 3 PeV iron-initiated air shower. The muons are indicated by grey dots, those passing through the detector stations (grey squares, those with gradient fill are not yet connected to the DAQ) are black while the shower-axis position is indicated by red cross. For the scale a large square is 50×50 m^2.

All in all, EMMA differs from the previous underground measurements by two key elements: i) taking the data at the shallow depth (∼75m vs. ∼1000m) and ii) recording lateral muon distributions for each shower.

2. Experimental setup

The main infrastructure of EMMA is now completed including 11 detector stations at the depth of 75 metres (50 GeV muon cutoff energy) in the Pyhäsalmi mine, Finland. Currently the stations are being successively instrumented and connected to the data acquisition system. Fig. 2 shows the layout of the experiment. It has been adopted to the available tunnel network in the mine and reflects the limited detector coverage.

EMMA employs three different types of detectors. The bulk area is covered with the former LEP-DELPHI MUBs (or planks) [9] which are drift chambers filled with an Ar(92%):CO_2(8%)-mixture. Each plank consists of seven position sensitive chambers (365×20 cm^2, 2 cm thick) arranged in lengthwise half-overlapping groups of 3 + 4 (called Y and X, respectively). Thus the active area of a plank is 2.9 m^2. The position resolution (σ, or standard deviation) is better than $\pm$1 cm^2 (see Fig. 3 for details) and the total area of planks is approximately 240 m^2.

The gas mixture is delivered from the ground via a $\sim$ 100 metres long pipeline through the rock. Due to the large total volume of drift chambers the gas consumption is rather high approaching 10 litres a minute (NTP). Thus the pipeline is both safety and practical issue because there is no need to transport rather large amounts of gas through the mine caverns.

The second type of EMMA-detectors is a plastic scintillation detector, or SC16 [10]. The SC16-detectors are designed and manufactured by the INR/RAS, Moscow. One SC16 detector consists of 4×4 individual 12×12×3 cm^3 pixels. The active area of SC16 is thus 0.5×0.5 m^2 and the total number of SC16s is 72 (or 18 m^2). The SC16-detectors are placed in the three central stations (C, F and G in Fig. 2). As the total number of individual pixels is 1152 the SC16 setup is an excellent tool for detailed muon multiplicity studies. Furthermore, the time resolution is good (with σ better than 2 ns, see Fig. 4 for details) and therefore SC16s provide a useful and independent initial guess for the shower arrival angles and improve muon tracking.

The third detector type is the Limited Streamer Tube (or LST) [11]. LSTs are CO_2-filled position sensitive detectors dismantled from the KASCADE-Grande experiment. One module has an area of 2.9 m^2 (1.0×2.9 m^2). The number of modules is 60 and the total area is $\sim$ 174 m^2. The detectors are designed for muon tracking and the pixel size of one LST-module is 2×8 cm^2. The CO_2-consumption of the LSTs is small, or less than 1% that of planks.

Our data acquisition uses the VME system. One VME unit is placed on each arm (currently in stations C, F and G) and all are connected together via optical connections.

EMMA employs two kinds of detector stations. The tracking stations (C, F and G) consist of three parallel and horizontal layers of five side-by-side planks (area 3650×4225 mm^2 or 15.4 m^2) with vertical distances of 1125 mm. In addition there is one layer of SC16s (24 pieces) and one of LSTs (5×2.9 m^2 or 14.5 m^2). The tracking is important for the muon cutoff energy estimate (cutoff energy increases with rock overburden, which in turn increases with zenith angle) and the angular resolution is better than one degree for single muons.

The outer detector stations, or sampling stations extend up to 30 metres from the central ones and host only two layers of planks or LSTs arranged similarly to those in the tracking stations. All stations employ muon tracking but tracking in the sampling stations is used solely for background reduction due to poorer angular resolution than that of tracking stations.

3. Performance - two examples

While EMMA is not yet fully operational, the test measurements are already running. These tests are important for the analysis and calibration software development but also improve our understanding on the detector performance underground. The main tool for any analysis is obviously muon tracking and the good position resolution of planks and small systematic errors in positions are essential part of it. The muon detection efficiencies are also estimated using tracking and are typically around 90% and are measured online (see text below).

One way to estimate these errors is to use residuals $\Delta\text{pos} = \text{pos}_{track} - \text{pos}_{muon}$ where pos_{track} is the track position calculated for each measured muon position and pos_{muon} is the measured muon position. This is illustrated in Fig. 3 where these residuals are plotted as sums of all X and Y chambers in all three detector layers, i.e. six sums of 20 and 15 chambers, respectively, for the delay-line direction and three sums of X-Y coincidences in the drift direction.

As shown in Fig. 3 the position resolutions (or residuals) are good and similar for all data sets. Characteristic numbers, like width (σ) and centroid (μ) are $\sigma < 7$ mm and $|\mu| < 1$ mm for

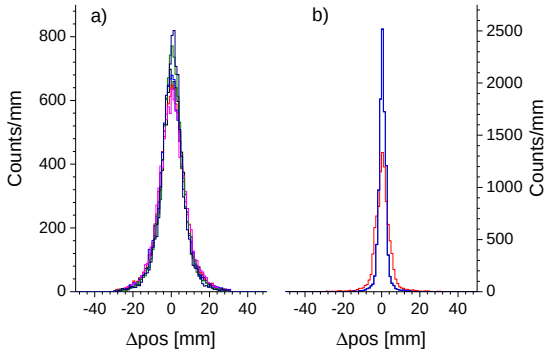

Figure 3. Measured position resolutions (residuals $\Delta\text{pos} = \text{pos}_{track} - \text{pos}_{muon}$) in the delay-line direction (a) and the drift direction (b). The single-muon data were recorded in 12 hours. See text for details.

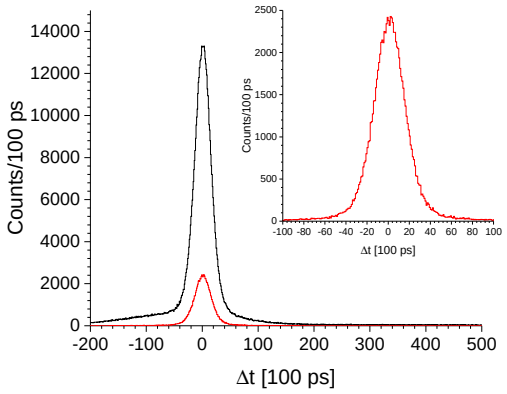

Figure 4. Measured time differences between two parallel sets of SC16s $\approx$ 1.1 m apart. The peaks are the sum of all coincidences (black curve) and those also with at least one muon track detected by drift chambers (red curve and inset). See text for details.

the delay-line directions and $\sigma < 4$ mm and $|\mu| < 1$ mm for those of the drift, respectively.

Another example is the timing properties of SC16s. The time resolution and systematic errors in measured time differences were investigated using a simple setup: two parallel sets of SC16s with $8{\times}16 = 128$ and $24{\times}16 = 384$ pixels on lower and upper levels (or 2 m^2 and 6 m^2), respectively, $\approx$ 1.1 metres apart. Thus the numbers of individual pixels were rather large and the setup was well suited for the timing studies and calibrations (i.e. delay matching).

The trigger logic was also simple: an unambiguous "track" of two pixels was required (i.e. one fired pixel on both levels) with the squared distance of $r^2 = x^2 + y^2 + z^2$ and the muon velocity assumed to be the speed of light for correcting the TOF. The measured time differences are shown in Fig. 4 for all coincidences and for those also with at least one muon track detected by drift chambers. These demonstrate that the timing properties of SC16s are excellent with $\sigma \approx 1.5$ ns and $|\mu| < 100$ ps for the sum.

The muon detection efficiencies were investigated with another setup prior to the present study by arranging 2×2 SC16s in five overlapping levels and requiring coincidences in vertical pixels (minimum 4 out of 5). The study revealed that the efficiencies are typically better than 95%. In the analysis the efficiencies of individual pixels as well as those of the drift chambers are used as an input.

4. Multi muons - one example

In a simplified picture the composition analysis is based on two variables: the measured muon multiplicities in each station and the arrival angles. The latter are important for the rock overburden (i.e. losses in muons as the larger the zenith angle the more rock to be penetrated by muons) while the muon multiplicities must be measured as accurately as possible because those are used as an input for reconstructing the muon lateral distributions which provide data for the primary shower energy and composition analysis. Therefore the corrections for losses due to muon detection efficiencies must be as accurate as possible (the simulated muon multiplicities are corrected for measured muon detection efficiencies and compared to those of measured multiplicities).

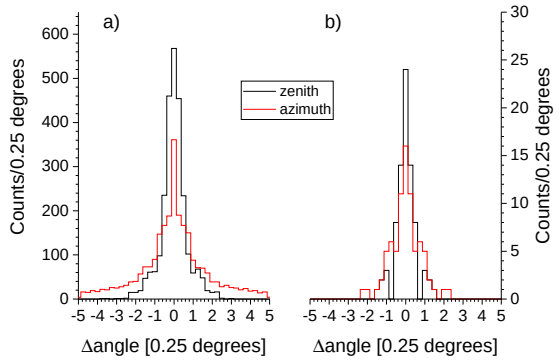

Figure 5. Measured angular (zenith and azimuth) differences between average angles and individual 5-hit (a) and 6-hit (b) tracks within an event. The data were recorded within ≈ 400 hours. See text for details.

Table 1. Measured numbers of muon tracks for each multiplicity used in Fig. 5.

Multiplicity	'5-hit'	'6-hit'	Sum
1	2049036	456021	2360211
2	1204	40	73209
3	52	0	318
4	6	0	27
5	2	0	5
6	1	0	3
7	0	0	1
8	0	0	0
9	0	0	0
10	0	0	0

Some preliminary estimates for these two can be extracted using the data of just one tracking station. Fig. 5 shows the measured angular differences between average angles and those of individual '5-hit' and '6-hit' tracks (coincs. of X and Y chambers in two or three double layers, respectively, see Sect. 2 for details) for zenith and azimuth angles while the measured numbers of corresponding tracks are listed in table 1. As shown in the figure, the angular resolutions are better than one degree in all cases while 5-hit tracks dominate due to efficiency and geometrical reasons (three quarters of area are covered with both X and Y chambers while a quarter is solely X) as listed in table 1. The latter also explains the larger number of 5-hit tracks than those of 6-hits as there are many more multiplicity-larger-than-one events in the 5-hit tracks than those of 6-hits. However, the angular resolutions seem rather similar for both cases, as also expected.

5. Conclusions

In the present work we have evaluated the key parameters characterizing the performance of the EMMA tracking stations. The resolution values extracted during the test and calibration measurements fullfil the requirements for the full analysis and confirm that the concept and design of EMMA are sound. The low-multiplicity muon efficiencies are well understood while those of high muon multiplicities are currently being investigated. The study will be completed when a high-granularity scintillation array and limited streamer tubes will be added to all tracking stations during 2016.

References

[1] Apel W D *et al.* KASCADE-Grande Collaboration 2013 *Astroparticle Physics* **47** 54
[2] Cebula D *et al.* 1990 *Astrophys. J.* **358** 637
[3] Kasahara S M *et al.* 1997 *Phys. Rev. D* **55** 5282
[4] Avati V *et al.* 2003 *Astroparticle Physics* **19** 513
[5] Grupen C *et al.* 2003 *Nucl. Inst. Meth. in Phys. Res. A* **510** 190
[6] Aglietta M *et al.* EAS-TOP & MACRO Collaborations 2004 *Astroparticle Physics* **20** 641
[7] Heck D *et al.* 1998 *Report FZKA* **6019**
[8] Kuusiniemi P *et al.* 2011 *Astrophys. Space Sci. Trans.* **7** 93
[9] Aarnio P *et al.* DELPHI Collaboration 1991 *Nucl. Inst. Meth. in Phys. Res. A* **303** 233
[10] Akhrameev E V *et al.* 2009 *Nucl. Inst. Meth. in Phys. Res. A* **610** 419
[11] Antoni T, Bercuci A, Bozdog H, Haungs A, Mathes H J, Petcu M, Rebel H and Zagromski S 2004 *Nucl. Inst. Meth. in Phys. Res. A* **533** 387